Scripta Materialia 114 (2016) 93–97

Contents lists available at ScienceDirect

Scripta Materialia

journal homepage: www.elsevier.com/locate/scriptamat

Regular Article

# On the critical thickness for non-localized to localized plastic flow transition in metallic glasses: A molecular dynamics study

C. Zhong [a,b], H. Zhang [a,b,c], Q.P. Cao [a,b], X.D. Wang [a,b], D.X. Zhang [d], U. Ramamurty [a,b,e,f], J.Z. Jiang [a,b]

[a] International Center for New-Structured Materials (ICNSM), Laboratory of New-Structured Materials, State Key Laboratory of Silicon Materials, Zhejiang University, Hangzhou 310027, People's Republic of China
[b] Department of Materials Science and Engineering, Zhejiang University, Hangzhou, 310027, People's Republic of China
[c] Department of Chemical and Materials Engineering, University of Alberta, Edmonton, Alberta T6G 2V4, Canada
[d] State Key Laboratory of Modern Optical Instrumentation, Zhejiang University, Hangzhou 310027, People's Republic of China
[e] Department of Materials Engineering, Indian Institute of Science, Bangalore 560 012, India
[f] Center of Excellence for Advanced Materials Research, King Abdulaziz University, Jeddah 21589, Saudi Arabia

ARTICLE INFO

*Article history:*
Received 28 October 2015
Received in revised form 7 December 2015
Accepted 7 December 2015
Available online 19 December 2015

*Keywords:*
Metallic glass
Molecular dynamic simulation
Mechanical
Behavior
Size effect

ABSTRACT

Molecular dynamics simulations were employed to investigate the specimen thickness-dependent tensile behavior of a series of $Cu_xZr_{100-x}$ ($x = 20, 40, 50, 64$ and 80 at.%) metallic glass (MG) films, with a particular focus on the critical thickness, $t_c$, below which non-localized plastic flow takes place. The simulation results reveal that while the transition occurs in all the alloys examined, $t_c$ is sensitive to the composition. We rationalize $t_c$ by postulating that the strain energy stored in the sample at the onset of plastic deformation has to be sufficient for the formation of shear bands. The composition-dependence of $t_c$ was found to correlate with the average activation energy of the atomic level plastic deformation events.



Size-dependence of plastic deformation behavior of materials is a topic of current research within the materials engineering discipline [1–18]. Within it, "how the mechanical behavior of metallic glasses (MGs) changes as the size of the specimens is reduced?" and "what are the mechanics/mechanisms responsible?" are questions for which answers are being sought actively by the MG community. At macroscopic scale, and at sufficiently low temperatures, plastic flow in MGs, if and when it occurs, manifests as localized flow into narrow regions that are often referred to as shear bands. Preceding the shear band formation, flow occurs through the activation of shear transformation zones (STZs) [19], which are clusters of atoms undergoing collective shear in order to relax the imposed stress. Prior studies, especially those performed on micro/nanopillars in compression, have shown that a transition from localized flow to continued non-localized deformation occurs when the specimen size is sufficiently small. A number of explanations are offered in literature for the observed transition, most of which are similar –conceptually– to the Griffith's criterion for fracture [9–18]. Essentially, they argue that the change in the deformation mode occurs only when the reduction in the elastic strain energy that occurs with the shear band propagation is larger than the effective surface energy increase due to the formation of a shear band. Since elastic strain energy stored in a stressed solid is proportional to the size of the sample itself, larger than a certain critical sized samples will necessarily undergo a deformation mode transition. However, a shear band is a three-dimensional volume within the specimen that undergoes plastic deformation rather than a two-dimensional crack with well defined surfaces. Thus, question on the appropriateness of using the Griffith-like criterion arises, which we seek to address in this paper. Since precise fabrication of extremely small sized specimens, with systematic variation of specimen size while keeping the thermal history invariant, is rather difficult if not impossible, we resort to atomistic simulations to study the size-dependent tensile deformation behavior of MGs, and then critically examine the deformation mode transition in them.

MD simulations of $Cu_{20}Zr_{80}$, $Cu_{40}Zr_{60}$, $Cu_{50}Zr_{50}$, $Cu_{64}Zr_{36}$ and $Cu_{80}Zr_{20}$ MGs were performed utilizing LAMMPS [20], employing the embedded-atom method potentials developed by Mendelev et al. [21], with the following sequential steps: (1) one big sample with a size of 28.2 nm ($x$) × 56.4 nm ($y$) × 5.6 nm ($z$) and ~500,000 atoms is generated. The detailed procedure of "melt–quench–duplicate" is similar to the procedures described in the literature [22,23]: after a cubic cell with five different compositions melted at 2000 K and zero pressure for two ns to ensure homogeneity, during which periodic boundary conditions (PBCs) were applied to all three dimensions, the cell was quenched from 2000 to 50 K over 19.5 ns at a cooling rate of $10^{11}$ K/s. The final

*E-mail address:* jiangjz@zju.edu.cn (J.Z. Jiang).

http://dx.doi.org/10.1016/j.scriptamat.2015.12.012
1359-6462/

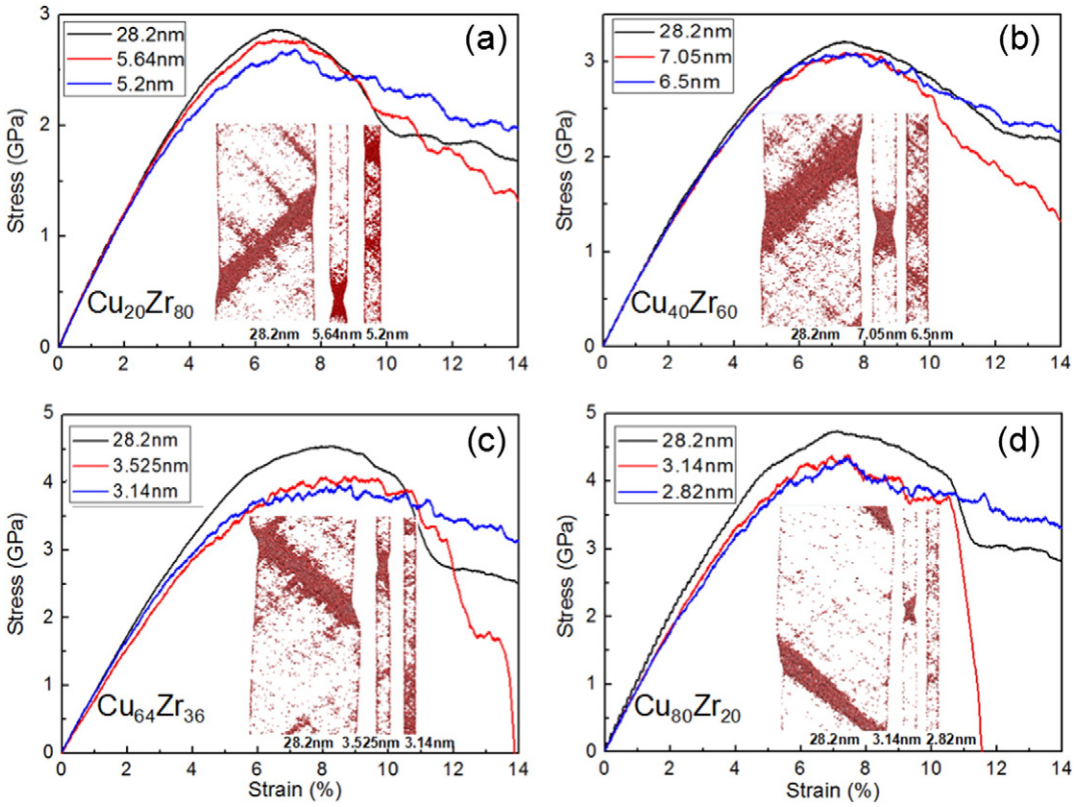


**Fig. 1.** Stress–strain curves and deformation maps for Cu–Zr MG films at three different thicknesses. (a) $Cu_{20}Zr_{80}$ MG, (b) $Cu_{40}Zr_{60}$ MG, (c) $Cu_{64}Zr_{36}$ MG, and (d) $Cu_{80}Zr_{20}$ MG.

dimensions of the cubic cell were measured to be $5.6 \times 5.6 \times 5.6$ nm$^3$. It was then duplicated to a big sample with a size of 28.2 nm ($x$) × 56.4 nm ($y$) × 5.6 nm ($z$). (2) After 1 ns relaxation at 50 K of the big sample, films with various thicknesses, $t$, were cut from the central part of the big sample along $x$ axis while the dimensions in $y$ and $z$ axes were not changed. (3) Subsequent to cutting, specimens were relaxed for 100 ps relaxation at 50 K. (4) All the films as well as the big specimen were tensile tested along $y$ direction at a constant strain rate of $1 \times 10^8$ s$^{-1}$ to a total strain of 14% at 50 K. It is important to note here that all the studied films were subjected to the same processing history and strain rate. Thus, the only variable, other than composition, in this campaign is the film thickness. During deformation, PBCs were imposed on $y$ and $z$ directions, while the free surface condition was applied to the $x$ direction, so that the deformed sample mimics a thin film. The time step for deformation was chosen as 1 fs. To visualize plastic shearing during deformation, the local shear invariant von Mises strain of each atom [24] in the sample was calculated using the equation: $\eta_i^{\text{Mises}} = \sqrt{\frac{1}{2}\text{Tr}(\eta - \eta_m\ \text{I})^2}$, where $\eta$ and $\eta_m$ are the local Lagrangian and hydrostatic strains for that atom, respectively. Atoms with $\eta_i^{\text{Mises}} \geq 0.2$ were termed as sheared atoms or "S-atoms" and were utilized to visualize the plastic deformation within the specimen. The region with a high density of "S-atoms" is identified as a shear band.

Fig. 1(a) shows stress–strain (SS) responses obtained on $Cu_{20}Zr_{80}$ MG with three different t. While all the SS curves exhibit a peak stress followed by softening with the exception of the 28.2 nm-thick film that exhibits a sharp drop after a strain of ~9%, an apparent characteristic of localized deformation, similar to that reported in literature [22,23]. Localization of flow was also confirmed by the deformation map, displayed in the inset of Fig. 1(a), wherein the formation of a prominent shear band can be seen. The SS response of the film with $t = 5.64$ nm is similar, and necking of the sample was observed, which indicates that localization of flow is still prevalent. When $t$ is further reduced to

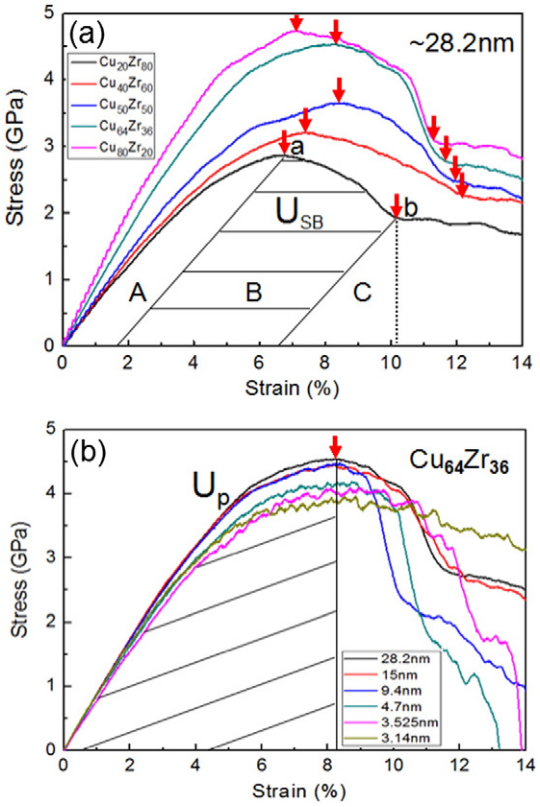


**Fig. 2.** (a) Stress–strain curves of five 28.2 nm-thick and schematic illustration of the procedure utilized for estimating $U_{SB}$. (b) Stress–strain curves of $Cu_{64}Zr_{36}$ MG with different thicknesses and schematic illustration of method utilized for computing $U_p$.